Stability of Beam Bridges under Bridge-Vehicle Interaction

AYOUB EL AMRANI[1], HAFID MATAICH[1], BOUCHTA EL AMRANI[1,*]
[1]Laboratory of Mathematics, Modeling and Applied Physics,
High Normal School, Sidi Mohamed Ben Abdellah University,
PB 5206 Bensouda 30040 Fez,
MOROCCO

**Corresponding Author*

Abstract: -In this paper, we provide an accurate and reliable formulation for simulating the interactions of both train/bridge subsystems and suitable for high-speed railway lines as well as for existing lines worldwide that are being renewed or modernized. We model the train as a series of suspended masses, taking into account the energy dissipation and the suspension system for each train vehicle. On the other hand, the bridge supporting the rails with irregular elevations will be modeled as an Euler-Bernoulli beam. The mathematical formulation of the interaction problem between the two subsystems requires the writing of two sets of equations, which interact with each other through contact forces. Using a one-dimensional finite element formulation, a series of equations are constructed by Modeling the beam structure. In addition, the suspended mass equations are first discretized using Newmark's finite difference formulas, which then reduce the degrees of freedom (DOF) of the vehicle to those of the bridge element. This solves the coupling problem between the two subsystems. The derived component is known as the vehicle/bridge interaction (VBI) element. On the other hand, an iterative procedure will be used subsequently to solve the non-linearity problem of the resulting system of differential equations. MATLAB programs provide results that identify the critical parameters influencing the bridge's dynamic stability.

Key-Words: - Beam bridge; Railway bridge stability; High-speed train; Suspended mobile mass; Bridge-vehicle interaction, beam vibration, iterative procedure; Newmark.

Received: July 2, 2023. Revised: February 24, 2024. Accepted: March 21, 2024. Published: May 13, 2024.

NOMENCLATURE

M_v	The flat rate mass of the bodywork	m	The mass per unit length of the beam
m_v	The mass of a train wheel	I	The moment of inertia of the beam
k_v	The stiffness of the suspension unit	L	The overall length of the beam
c_v	The damping of the suspension unit	x_c	The abscissa of the action of contact force
y_1, y_2	Displacements of wheel and bodywork nodes	k_B	The stiffness of the bridge ballast
$\dot{y}_1, \dot{y}_2$	Velocities of displacement of wheel and bodywork nodes	$r(x)$	Rail irregularity at abscissa x
$\ddot{y}_1, \ddot{y}_2$	Accelerations of displacement of wheel and bodywork nodes	F_c	The contact force between the two subsystems
v	The constant speed of the train	w_b	Transversal displacement of the beam
p	The total weight of the two mass units M_v and m_v	$\dot{w}_b$	The velocity of transversal displacement of the beam
E	The Young's modulus of the beam structure	$\ddot{w}_b$	Acceleration of transversal displacement of the beam
v	The Poisson's coefficient	N_c	Beam shape functions
Δy_1	Increment of wheel displacement	ΔW_b	Increment of bridge displacement
Δy_2	Increment of bodywork displacement	c_i	Coefficients of the β-Newmark method

1 Introduction

In recent years, the construction of high-speed railway tracks (TGV) and suspension bridges in various countries around the world has seen significant progress. This has given rise to several phenomena, among which the vibrational effects on bridges caused by the passage of these high-speed trains have become a subject of growing interest. Studies conducted by the authors [1], [2], [3], [4], [5], [6], [7] show that vehicle speed is one of the

factors, among others, affecting the transverse dynamic instability of the bridge. Dynamic bridge-vehicle interactions have been examined by several researchers in the literature, [8], [9], [10], [11], addressing the effects influencing the dynamic behavior of bridges when interacting with moving vehicles. These studies model moving vehicles as mobile loads, moving masses, or suspended masses in motion, taking into account suspension mechanisms and energy dissipation associated with vehicles. More sophisticated models that consider various dynamic properties of vehicles or train cars have also been implemented in the study of vehicle-bridge interactions, [12]. In this book, and more specifically in chapters 9 and 10, the authors delve into the Modeling of 2D and 3D interaction problems.

The treatment of dynamic interactions in a vehicle-bridge system requires the determination of two sets of motion equations, one for the bridge structure (the stationary subsystem) and the other to model the moving vehicle structure (the moving subsystem) as presented in this work, [13]. The interaction between the two subsystems is achieved through contact forces existing at the contact points of the two subsystems. Due to these forces, both sets of equations will be coupled and nonlinear. However, the contact position varies in time and space, so the mass, damping, and stiffness matrices, which are functions of the contact forces, must be reformulated at each time step in a time-domain analysis. Solving this system of coupled differential equations requires us to adopt an iterative procedure based on time integration using β-Newmark finite difference formulas (which are classical methods with average acceleration and unconditionally stable associated with specific values of γ=0.5 and β=0.25; for more details on this algorithm, [14]).

In this study, we employ a dynamic condensation approach to solve vehicle-bridge interaction problems. This method has been used in the literature, as described in reference, [12], where the reduction scheme was used to condense the vehicle's degrees of freedom to the associated degrees of freedom of the bridge. However, if we need to obtain the response of the vehicles, which serves as a reference for assessing passenger comfort, we cannot rely on the two approaches mentioned above to obtain accurate solutions because approximations have been made to connect the vehicle's degrees of freedom (slave) to those of the bridge (master).

2 Mathematical Modeling of the Study Problem

Physical Modeling of the problem

The passage of a high-speed TGV train over a beam bridge produces mutual effects between the two subsystems, namely the vehicles on one side and the bridge on the other side. These effects are known as Vehicle Bridge Interaction (VBI) dynamics, [15]. In this paper, we examine the impact of these interactions on the dynamic response of the bridge. The proposed physical model for the bridge-vehicle interaction problem in this study is as follows: the bridge is represented by an Euler-Bernoulli beam structure (small deformations and negligible shear effects) of length L, and the train in motion at a constant speed v is approximated by a sequence of suspended mass units (N wheels), distributed in pairs for each front and rear bogie of the wagon, as shown in Figure 1.

In this study, we propose not to consider the effect of the variation in the distance between the wheels on the dynamic response of the bridge. Therefore, we assume that all the wheels of the train are separated by regular distances (d_v), as shown in the diagram in Figure 2. Consequently, each suspended mass unit represents each train carriage's front or rear half.

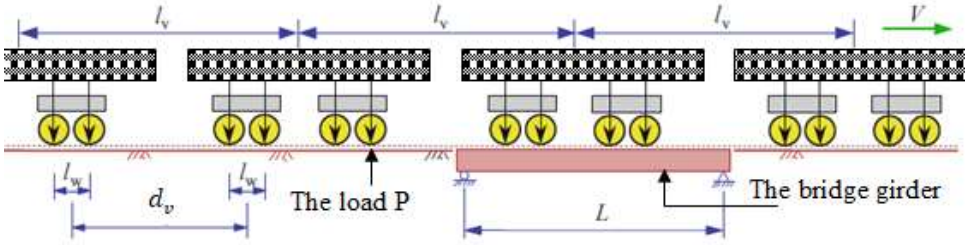

Fig. 1: A beam of length L under the loading of a succession of train cars

Ayoub El Amrani,
Hafid Mataich, Bouchta El Amrani

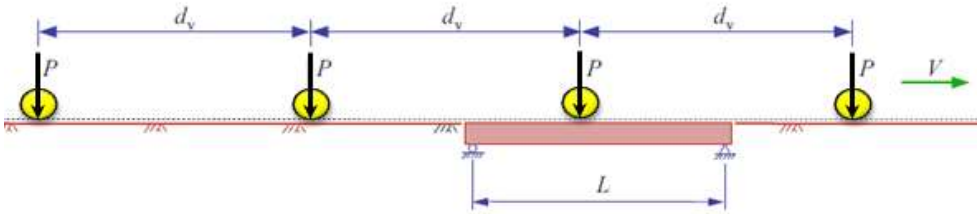

Fig. 2: Idealization of the load on the beam by mobile loads separated by a uniform distance d_v

2.1 Vehicle Dynamics

We consider a suspended mass model consisting of two nodes, with one node associated with each of the two concentrated masses. Similarly, the vertical displacements of the two masses are denoted by the coordinates $\{y\}^T = \{y_1, y_2\}$. The equations of motion for this model can be expressed according to the fundamental principles of dynamics, as described in [7].

$$\begin{bmatrix} m_v & 0 \\ 0 & M_v \end{bmatrix}\begin{Bmatrix} \ddot{y}_1 \\ \ddot{y}_2 \end{Bmatrix} + \begin{bmatrix} c_v & -c_v \\ -c_v & c_v \end{bmatrix}\begin{Bmatrix} \dot{y}_1 \\ \dot{y}_2 \end{Bmatrix} + \begin{bmatrix} k_v & -k_v \\ -k_v & k_v \end{bmatrix}\begin{Bmatrix} y_1 \\ y_2 \end{Bmatrix} = \begin{Bmatrix} p + F_c \\ 0 \end{Bmatrix} \quad (1)$$

F_c is the contact force between the two models representing the vehicle and that of the bridge, which is given by the following expression:

$$F_c = k_B(\{N_c\}^T\{w_b\} + r_c - y_1) \quad (2)$$

The Hermitian shape function evaluated at the point of contact force application, x_c, is $\{N_c\} = \{N(x_c)\}$, and the nodal displacement vector $\{w_b\}^T = \left\{w_{b1}, \frac{\partial w_{b1}}{\partial x}, w_{b2}, \frac{\partial w_{b2}}{\partial x}\right\}$ of the active element $[x_{i-1}, x_i]$ of the beam. For more details regarding the beam finite element, [16]. Finally, $r_c = r(x_c)$ represents the irregularity of the rail which will be dealt with in section 6.3 and its expression is given later by eq. (34). Let $\{\Delta y\}$ be the increment of transverse displacement of the suspended mass unit, then:

$$\{y\}_{t+\Delta t} = \{y\}_t + \{\Delta y\} \quad (3)$$

By substituting equation (3) into equation (1), we obtain a temporal recurrence relation of the following form:

$$\begin{bmatrix} m_v & 0 \\ 0 & M_v \end{bmatrix}\begin{Bmatrix} \ddot{y}_1 \\ \ddot{y}_2 \end{Bmatrix}_{t+\Delta t} + \begin{bmatrix} c_v & -c_v \\ -c_v & c_v \end{bmatrix}\begin{Bmatrix} \dot{y}_1 \\ \dot{y}_2 \end{Bmatrix}_{t+\Delta t} + \begin{bmatrix} k_v + k_B & -k_v \\ -k_v & k_v \end{bmatrix}\begin{Bmatrix} \Delta y_1 \\ \Delta y_2 \end{Bmatrix}_{t+\Delta t} = \begin{Bmatrix} p + k_B(\{N_c\}^T\{w_b\} + r_c) \\ 0 \end{Bmatrix}_{t+\Delta t} - \begin{bmatrix} k_v + k_B & -k_v \\ -k_v & k_v \end{bmatrix}\begin{Bmatrix} y_1 \\ y_2 \end{Bmatrix}_t \quad (4)$$

Based on the β-Newmark finite difference scheme [17], as follows:

$$\begin{aligned} \{\ddot{y}\}_{t+\Delta t} &= c_0\{\Delta y\} - c_2\{\dot{y}\}_t - c_3\{\ddot{y}\}_t \\ \{\dot{y}\}_{t+\Delta t} &= \{\dot{y}\}_t + c_6\{\ddot{y}\}_t + c_7\{\ddot{y}\}_{t+\Delta t} \end{aligned} \quad (5)$$

With

$$\begin{aligned} c_0 &= \frac{1}{\beta\Delta t^2}, \quad c_1 = \frac{\gamma}{\beta\Delta t}, \quad c_2 = \frac{1}{\beta\Delta t} \\ c_3 &= \frac{1}{2\beta} - 1, \quad c_4 = \frac{\gamma}{\beta} - 1, \quad c_5 = \frac{\Delta t}{2}\left(\frac{\gamma}{\beta} - 2\right) \\ c_6 &= \Delta t(1-\gamma), \quad c_7 = \gamma\Delta t \end{aligned} \quad (6)$$

We manipulate the equations of the system Eq. (4) and substituting the expressions of the equation Eq. (5), we obtain the following equivalent stiffness equations:

$$[D]\begin{Bmatrix} \Delta y_1 \\ \Delta y_2 \end{Bmatrix} = \begin{Bmatrix} p + k_B(r_c + \{N_c\}^T\{w_b\}) \\ 0 \end{Bmatrix}_{t+\Delta t} - \begin{Bmatrix} q_{s1} \\ q_{s2} \end{Bmatrix}_t - \begin{Bmatrix} q_{e1} \\ q_{e2} \end{Bmatrix}_t \quad (7)$$

In order to simplify the writing of the expressions, we set:

$$D = det[D] = \begin{vmatrix} k_v + k_B + c_0 m_v + c_1 c_v & -k_v - c_1 c_v \\ -k_v - c_1 c_v & k_v + c_0 M_v + c_1 c_v \end{vmatrix} \quad (8)$$

And also:

$$\begin{Bmatrix} q_{s1} \\ q_{s2} \end{Bmatrix}_t = \begin{bmatrix} k_v + k_B & -k_v \\ -k_v & k_v \end{bmatrix}\begin{Bmatrix} y_1 \\ y_2 \end{Bmatrix}_t \quad (9)$$

$$\begin{Bmatrix} q_{e1} \\ q_{e2} \end{Bmatrix}_t = -\begin{Bmatrix} m_v(c_2\dot{y}_1 + c_3\ddot{y}_1) \\ M_v(c_2\dot{y}_2 + c_3\ddot{y}_2) \end{Bmatrix} + \begin{Bmatrix} -c_v[c_4(\dot{y}_1 - \dot{y}_2) + c_5(\ddot{y}_1 - \ddot{y}_2)] \\ -c_v[c_4(\dot{y}_2 - \dot{y}_1) + c_5(\ddot{y}_2 - \ddot{y}_1)] \end{Bmatrix}_t \quad (10)$$

Finally, the vertical displacement increments of the suspended mass unit $\{\Delta y\}^T = \{\Delta y_1, \Delta y_2\}$ can be written in terms of the bridge displacement $\{w_b\}$ at time $t + \Delta t$, as follows:

$$\begin{Bmatrix} \Delta y_1 \\ \Delta y_2 \end{Bmatrix} = -\frac{1}{D}\begin{Bmatrix} (k_v + c_0 M_v + c_1 c_v) \\ (k_v + c_1 c_v) \end{Bmatrix} \times \begin{Bmatrix} \left(p + k_B\left(r_{c,t+\Delta t} + \{N_c\}^T\{w_b\}_{t+\Delta t}\right)\right) \\ \left(p + k_B\left(r_{c,t+\Delta t} + \{N_c\}^T\{w_b\}_{t+\Delta t}\right)\right) \end{Bmatrix} - \frac{1}{D}\begin{Bmatrix} c_0 M_v(q_{s1} + q_{e1}) \\ (q_{s1} + q_{e1})(c_0 m_v + k_B) + \end{Bmatrix}_t - \frac{1}{D}\begin{Bmatrix} (q_s + q_e)(k_v + c_1 c_v) \\ (q_s + q_e)(k_v + c_1 c_v) \end{Bmatrix} \quad (11)$$

To simplify, we always assume:

$$\begin{Bmatrix} q_e = q_{e1} + q_{e2} \\ q_s = q_{s1} + q_{s2} \end{Bmatrix} \quad (12)$$

2.2 Bridge Dynamics

We adopt a classical Euler-Bernoulli approach in the plane which assumes small deformations therefore we neglect all transverse shear deformations. So, the beam element (Figure 3) will be characterized by two degrees of freedom DOF per node, a deflection $w_b(x)$ in the x-y plane and a rotation $\partial w_b/\partial x$ around the z-axis. The beam dynamics is approximated using Hermite interpolation functions (the N_i functions are listed in Appendix as A-1), which are able to give an exact nodal solution in the finite element (super-convergent element).

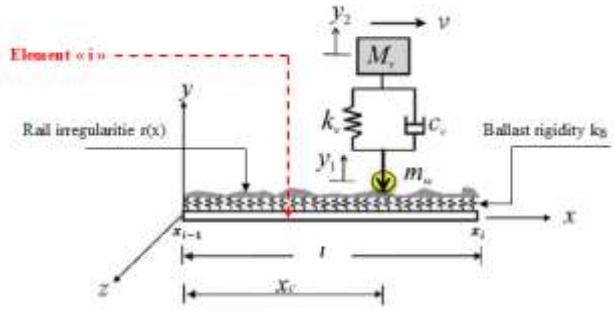

Fig. 3: The proposed vehicle-bridge interaction elementary element is a mass suspended from a beam

Using Hamilton's energy principle, [18], the bridge element that reacts with the suspended mass unit is governed by the following motion equations:

$$[m_b]\{\ddot{w}_b\} + [c_b]\{\dot{w}_b\} + [k_b]\{w_b\} = \{p_b\} - \{N_c\}F_c \quad (13)$$

Where, $[m_b], [c_b]\ and\ [k_b]$ are respectively the mass, damping and stiffness matrices of the bridge element, and $\{p_b\}$ represents the external nodal load applied to the element. In the case where the bridge element behaves as a two-dimensional rigid beam element, we assign four DOFs for each element (one translation and one rotation for each node). The beam damping in this case is assumed to be of Rayleigh type, so the matrix $[c_b]$ can be expressed as a linear combination of the mass and stiffness matrices, [19]. The matrix $[m_b]$, $[k_b]$ and the damping $[c_b]$, are presented in Appendix A-2, A-3 and A-4.

Let $\{\Delta w_b\}$ be the transverse displacement increment of the beam element, then after the time increment Δt:

$$\{w_b\}_{t+\Delta t} = \{w_b\}_t + \{\Delta w_b\} \quad (14)$$

By substituting equation Eq. (14) into the motion equation Eq. (13), the motion's equations of bridge can be expressed in an incremental form.

$$\begin{aligned}&[m_b]\{\ddot{w}_b\}_{t+\Delta t} + [c_b]\{\dot{w}_b\}_{t+\Delta t} + \\ &([k_b] + k_B\{N_c\}\{N_c\}^T)\{\Delta w_b\} \\ &= \{p_b\}_{t+\Delta t} - k_B(r_c - y_1)_{t+\Delta t}\{N_c\} \\ &-([k_b] + k_B\{N_c\}\{N_c\}^T)\{w_b\}_t \end{aligned} \quad (15)$$

3 The Condensed Equation of the Bridge (Equation of the VBI System)

Equation Eq. (15) shows the coupling between the two subsystems via the displacement of the suspended mass $y_{1,t+\Delta t}$ on the right side of the equal sign. However, the other terms are known, such as the external nodal load $\{p_b\}_{t+\Delta t}$, which is known at the last time step, just like the displacement of the bridge element $\{w_b\}_t$. In order to decouple the equations of the two sub-systems, we assumed that $\{y_1\}_{t+\Delta t} = \{y_1\}_t + \{\Delta y_1\}$, using the expression of $\{\Delta y_1\}$ from equation Eq. (11). In this way, we obtain, from equation Eq. (15), the condensed equations of motion for the beam element at time $t + \Delta t$, considering the effect of the suspended mass unit interaction. Therefore, the degrees of freedom (DOF) of the vehicle are condensed to those of the bridge elements in contact, [20].

$$\begin{aligned}&[m_b]\{\ddot{w}_b\}_{t+\Delta t} + [c_b]\{\dot{w}_b\}_{t+\Delta t} + [\bar{\bar{k}}_b]\{\Delta w_b\} \\ &\quad = \{p_b\}_{t+\Delta t} + \{p_w\}_{t+\Delta t} - \{f_s\}_t - [\bar{\bar{k}}_b]\{w_b\}_t \end{aligned} \quad (16)$$

With, $[\bar{\bar{k}}_b]$ is the stiffness matrix of the condensed system.

$$\begin{aligned}[\bar{\bar{k}}_b] &= [k_b] + k_B\frac{c_0}{D}[(M_v + m_v)(k_v + c_1c_v) \\ &\quad + c_0M_vm_v]\{N_c\}\{N_c\}^T \end{aligned} \quad (17)$$

The load forces induced by the wheels, including contributions from rail irregularities and ballast stiffness.

$$\begin{aligned}\{p_w\}_{t+\Delta t} &= -k_B[r_{c,t+\Delta t} - (p + k_Br_{c,t+\Delta t}) \\ &\quad \times (k_v + c_0M_v + c_1c_v)/D]\{N_c\} \end{aligned} \quad (18)$$

The resistance forces associated with the suspended mass unit:

$$\begin{aligned}\{f_s\}_t &= k_B[(q_{s1,t} + q_{e1,t})c_0M_v/D + \\ &\quad (q_{s,t} + q_{e,t})(k_v + c_1c_v) - y_{1,t}]\{N_c\} \end{aligned} \quad (19)$$

The assembly of the interaction problem between the two subsystems requires a repetitive loop over all the elements interacting with the suspended mass (the elements denoted as VBI Eq.

(16)), as well as over the elements that do not interact with the vehicle. Therefore, the overall system of equations of motion for the two interacting subsystems is:

$$[M_b]\{\ddot{W}_b\}_{t+\Delta t} + [C_b]\{\dot{W}_b\}_{t+\Delta t} + [K_b]\{\Delta W_b\}_{t+\Delta t} = \{P_b\}_{t+\Delta t} - \{F_b\}_t \quad (20)$$

Where $\{W_b\}_{t+\Delta t}$ denotes all the displacements of all the nodes of the beam representing the bridge at time $t+\Delta t$, and $\{\Delta W_b\}$ represents the displacement increments of the bridge from time t to $t+\Delta t$, with:

$$\{W_b\}_{t+\Delta t} = \{W_b\}_t + \{\Delta W_b\} \quad (21)$$

The external nodal loads $\{P_b\}_{t+\Delta t}$ and the resisting forces $\{F_b\}_t$ on the right side of equation Eq. (20) are constructed as follows:

$$\begin{aligned}\{P_b\}_{t+\Delta t} &= \sum_{e=1}^{Elements}(\{p_b\}_{t+\Delta t} + \{p_w\}_{t+\Delta t}) \\ \{F_b\}_t &= \sum_{e=1}^{Elements}(\{f_s\}_t + [\bar{\bar{k}}_b]\{w_b\}_t)\end{aligned} \quad (22)$$

The damping matrix [C_b] is constructed using the procedure based on the assumption described in Appendix A.

1. Solving the resulting equation (equivalent stiffness equation).

First, the acceleration $\{\ddot{W}_b\}$ and the velocity $\{\dot{W}_b\}$ of the bridge can be related to the displacement increments $\{\Delta W_b\}$ between the time instants $t+\Delta t$ and t using $\beta - Newmark$ type finite difference formulas, as follows:

$$\begin{aligned}\{\ddot{W}_b\}_{t+\Delta t} &= c_0\{\Delta W_b\} - c_2\{\dot{W}_b\}_t - c_3\{\ddot{W}_b\}_t \\ \{\dot{W}_b\}_{t+\Delta t} &= \{\dot{W}_b\}_t + c_6\{\ddot{W}_b\}_t + c_7\{\ddot{W}_b\}_{t+\Delta t}\end{aligned} \quad (23)$$

By substituting the expressions Eq. (23) into the equation of the system Eq. (20), the final equation can be transformed into the following equivalent stiffness equations:

$$\left[\bar{\bar{K}}_b\right]_{t+\Delta t}\{\Delta W_b\} = \{P_b\}_{t+\Delta t} - \{\bar{\bar{F}}_b\}_t \quad (24)$$

With,

$$\left[\bar{\bar{K}}_b\right]_{t+\Delta t} = c_0[M_b] + c_1[C_b] + [K_b] \quad (25)$$

$$\{\bar{\bar{F}}_b\}_t = \{F_b\}_t + [M_b]\left(c_2\{\dot{W}_b\}_t + c_3\{\ddot{W}_b\}_t\right) + [C_b]\left(c_4\{\dot{W}_b\}_t + c_5\{\ddot{W}_b\}_t\right) \quad (26)$$

The matrix $\left[\bar{\bar{K}}_b\right]_{t+\Delta t}$ and the vector $\{P_b\}_{t+\Delta t}$ respectively representing the effective stiffness and the global external load are treated as constants during each time step.

4 Non-linearity Treatment (Iterative Procedure)

When a vehicle passes over a beam, there are mutual interactions between the two subsystems, the vehicle and the beam, through the contact force. This type of phenomenon is nonlinear, and its resolution requires an iterative procedure (such as the modified Newton-Raphson method) to eliminate the unbalanced force between the two subsystems. This iteration procedure is presented as the equivalent stiffness equation system of the interacting VBI system described by Eq. (24) must be modified, that is:

$$\left[\bar{\bar{K}}_b\right]_{t+\Delta t}\{\Delta W_b\}^i = \{P_b\}_{t+\Delta t} - \{\bar{\bar{F}}_b\}_{t+\Delta t}^{i-1} \quad (27)$$

The exponent «i» indicates the current iteration number. The resistant force vector in Eq (26) must be structured for iterations $i > 1$ as follows:

$$\{\bar{\bar{F}}_b\}_t^{i-1} = \{F_b\}_t^{i-1} + [M_b]\left(c_2\{\dot{W}_b\}_t^{i-1} + c_3\{\ddot{W}_b\}_t^{i-1}\right) + [C_b]\left(c_4\{\dot{W}_b\}_t^{i-1} + c_5\{\ddot{W}_b\}_t^{i-1}\right) \quad (28)$$

The initial conditions (i=1) are:

$$\{\bar{\bar{F}}_b\}_{t+\Delta t}^{ini} = \{\bar{\bar{F}}_b\}_t^{fin},\ \{W_b\}_{t+\Delta t}^{ini} = \{W_b\}_t^{fin} \text{ et } \{y\}_{t+\Delta t}^{ini} = \{y\}_t^{fin} \quad (29)$$

In each time increment, the displacement increments $\{\Delta W_b\}^i$ of the bridge, for all iterations performed, can be cumulated as:

$$\{W_b\}_{t+\Delta t}^i = \{W_b\}_{t+\Delta t}^{i-1} + \{\Delta W_b\}^i \quad (30)$$

Taking into account the loop of iterations, the acceleration and speed of the bridge can be obtained by:

$$\begin{aligned}\{\ddot{W}_b\}_{t+\Delta t}^i &= c_0\{\Delta W_b\}^i - c_2\{\dot{W}_b\}_{t+\Delta t}^{i-1} - c_3\{\ddot{W}_b\}_{t+\Delta t}^{i-1} \\ \{\dot{W}_b\}_{t+\Delta t}^i &= \{\dot{W}_b\}_{t+\Delta t}^{i-1} + c_6\{\ddot{W}_b\}_{t+\Delta t}^{i-1} + c_7\{\ddot{W}_b\}_{t+\Delta t}^i\end{aligned} \quad (31)$$

In the current incremental step iteration « i » the total vehicle response is calculated by:

$$\begin{aligned}\{y\}_{t+\Delta t}^i &= \{y\}_{t+\Delta t}^{i-1} + \{\Delta y\}^i \\ \{\ddot{y}\}_{t+\Delta t}^i &= c_0\{\Delta y\}^i - c_2\{\dot{y}\}_{t+\Delta t}^{i-1} - c_3\{\ddot{y}\}_{t+\Delta t}^{i-1} \\ \{\dot{y}\}_{t+\Delta t}^i &= \{\dot{y}\}_{t+\Delta t}^{i-1} + c_6\{\ddot{y}\}_{t+\Delta t}^{i-1} + c_7\{\ddot{y}\}_{t+\Delta t}^i\end{aligned} \quad (32)$$

5 Numerical Results and Interpretations

The two subsystems interact with each other, as presented in Figure 1, and will be roughly

characterized by the coefficients and parameters listed in Table 1.

5.1 Validation and Limitations

First, let's examine the parameters presented in Table 1, by setting the vehicle parameters $k_v, m_v \; and \; c_v$ to zero, in this situation, all loads passing through the beam are considered mobile loads. On the other hand, in the second case, by assigning zero values to the damping c_v and the mass m_v of all train wheels, as well as very high values to the stiffness of the vehicle k_v and the ballast k_B, the system obtained is a moving mass. The third case takes into account all the real properties of the bridge and the vehicle described by a suspended mass. In all three cases, we consider only the contribution of the first vibration mode of the beam.

Let's start with a numerical evaluation of the theoretical formulation proposed above, validating the importance of treating non-linearity. We consider a situation corresponding to the first case (mobile load) with two loading scenarios defined by the ratio of the vehicle's mass to the beam's mass, denoted $\left.\frac{vehicle\ mass}{beam\ mass}\right|_{m_v=0}$, where the first scenario corresponds to M_v/m_bL being equal to 0.1%, and the second scenario to M_v/m_bL being equal to 10%. The static deflection of the beam, denoted W_0 is equal to 9.3200 mm.

In Table 2, we execute the iterative algorithm for handling non-linearity to determine the impact factor IF, defined as $W(L/2,t)/W_0$, over eight iterations. The current calculations are performed with a train speed of v equal to $261.26\ km/h$ and a fundamental frequency of the beam, denoted ω_1, of $34\ rad/s$. The speed parameter S_1 is defined as $\pi v/(\omega_1 L) = 0.3$.

Table 1. Parameters of the interaction problem, bridge structure, and suspended mass

Vehicle-related settings	M_v	The flat rate mass of the bodywork	5750	kg
	m_v	The mass of a train wheel	0.00	kg
	k_v	The rigidity of the suspension unit	1595	kN/m
	c_v	The damping of the suspension unit	0.00	$kN.\frac{s}{m}$
	v	The constant speed of the train	100	km/h
	p	The total weight of the two mass units M_v and m_v	$(M_v + m_v)$	kg
	E	The Young's modulus of the beam structure	2.87	GPa
	v	The Poisson's ratio	0.2	m/s
Characteristics of the bridge structure	m	The mass per unit length of the beam	2303	kg/m
	I_z	The moment of inertia of the beam	2.90	m^4
	L	The overall length of the beam	25	m
	x_c	The abscissa of the point of contact force	V$* t$	m
	k_B	The rigidity of the bridge ballast	1595	$\frac{kN}{m}$
	$r(x)$	Rail irregularity	$r(x_c)$	m

Table 2. Digital recording of the « IF » impact factor for $M_v/m_bL = 0.001 \; and \; 0.1$ with $S_1 = 0.3$

Iteration « i »	Proposed model					[16]	[17]
	$M_v/m_bL = 0.1\%$		$M_v/m_bL = 10\%$				
	$W(0.5L,t)$	$W(0.5L,t)/W_0$	$W(0.5L,t)$	$W(0.5L,t)/W_0$			
1	9,2174	0,989	16,2168	1,7401		$\frac{M_v}{m_bL} = 0.1\%$	$\frac{M_v}{m_bL} = 10\%$
2	10,1494	1,089	20,8768	2,2411			
3	11,1933	1,201	23,8592	2,5600			
4	12,2185	1,311	26,6552	2,8601			
5	13,1505	1,411	28,8920	3,121			
6	14,1757	1,521	30,8492	3,3112			
7	14,4553	1,551	32,7132	3,5114			
8	14,6883	1,576	33,6452	3,6101		IF = 1.598	IF = 3.730

According to the results from the previous table, the impact factor observed at mid-span of the beam under the loading of the first situation, $M_v/m_bL = 0.1\%$ and $IF = 1.576$ is a result very

close to the reference, [21]. However, in the second loading situation with $M_v/m_bL = 10\%$, the obtained factor $IF = 3.6101$ requires more iterations for proper convergence, according to the results from [22]. From this observation, we notice a good correlation between the results obtained and those from the literature. Consequently, we can continue with the numerical manipulations using the theoretical approach adopted previously.

A graphical representation of processing algorithm convergence is shown in Figure 4. In this figure, the impact factor "IF" and the deviation $\left(W_b^i(L/2,t) - W_b^{i-1}(L/2,t)\right)/W_0$ are drawn in a histogram for each iteration in the case of $M_v/m_bL = 0.1\%$. Processing equation Eq. (27) returns a portion of the deflection used to correct the beam displacement increment $\{\Delta W_b\}$ with an accumulated deviation according to equation Eq. (30) $W_b^i(L/2,t) - W_b^{i-1}(L/2,t)$. In fact, from this illustration we see small corrections gained in each iteration (red bars) and an almost uniform distribution of "IF" values from iteration 1 to 8. So, incorporating the non-linearity treatment algorithm into the numerical analysis of the problem is not necessary.

Therefore, in the case of low ratios of $\frac{vehicle\ mass}{beam\ mass}\Big|_{m_v=0}$ (which indicates small deformations according to Euler-Bernoulli approximations), the incorporation of the non-linearity processing algorithm in the numerical analysis of the problem is not necessary.

Once again, the graphical representation of the convergence of the non-linearity processing algorithm is illustrated in Figure 5. In this figure, the impact factor « IF » and the difference $\left(W_b^i(L/2,t) - W_b^{i-1}(L/2,t)\right)/W_0$ are plotted for 8 iterations.

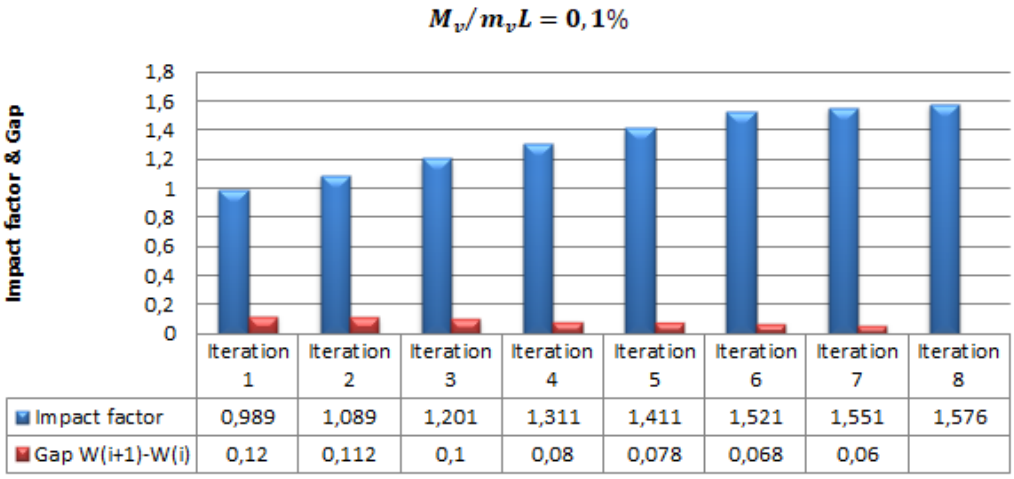

	Iteration 1	Iteration 2	Iteration 3	Iteration 4	Iteration 5	Iteration 6	Iteration 7	Iteration 8
Impact factor	0,989	1,089	1,201	1,311	1,411	1,521	1,551	1,576
Gap W(i+1)-W(i)	0,12	0,112	0,1	0,08	0,078	0,068	0,06	

Fig. 4: Graph shows the impact factor of the excited bridge in the case of $M_v/m_bL = 0.1\%$

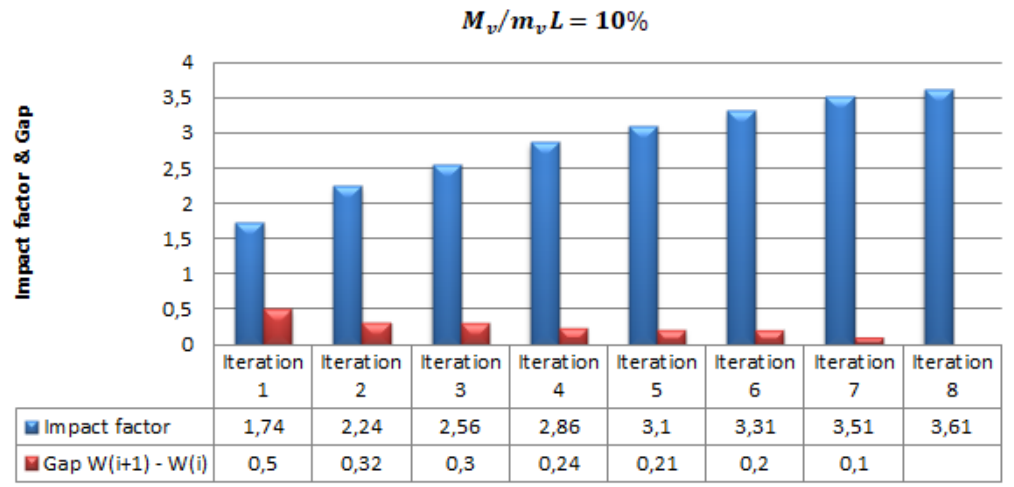

	Iteration 1	Iteration 2	Iteration 3	Iteration 4	Iteration 5	Iteration 6	Iteration 7	Iteration 8
Impact factor	1,74	2,24	2,56	2,86	3,1	3,31	3,51	3,61
Gap W(i+1) - W(i)	0,5	0,32	0,3	0,24	0,21	0,2	0,1	

Fig. 5: Graph shows the impact factor of the excited bridge in the case $M_v/m_bL = 10\%$

In contrast to the interpretation made for illustrations in the case of $M_v/m_bL = 0.1\%$. If the mass of the vehicle increases relative to that of the bridge, then the non-linear treatment of equation Eq. (27) is necessary, as the large deviations $W_b^i(L/2,t) - W_b^{i-1}(L/2,t)$ shown in Figure 5.

5.2 Results Related to a Single Suspended Mass

In this section, we investigate the dynamic response (lateral deflection) at the mid-point of the beam under the action of a suspended mass in uniform motion (constant train speed), considering only the contribution of the first mode of vibration of the beam. This situation corresponds to the second specific case of the suspended mass described in Section 6.1, complemented by the parameters from Table 1. This response is represented in Figure 6. As can be seen, the resulting dynamic response based on the VBI element Eq. (24) corresponds well to that of the first mode of the closed-form solution presented in [23].

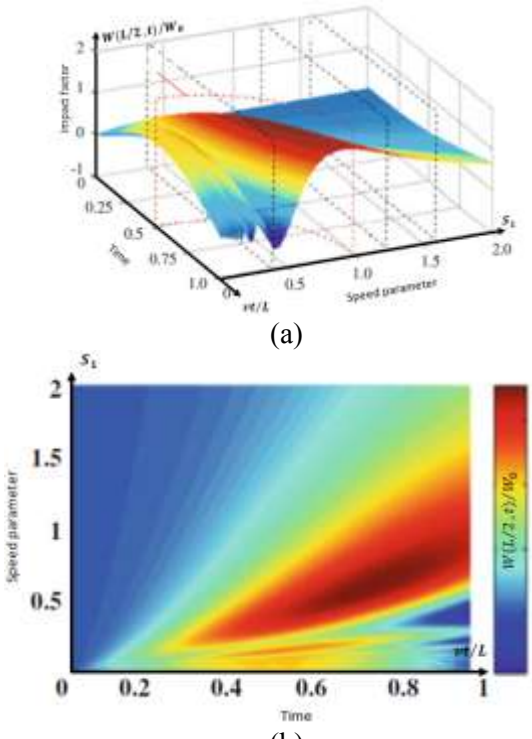

(a)

(b)

Fig. 6: The evolution of the impact factor of the beam (a) the special distribution (b) the planar distribution

The illustration of the relative displacement at mid-span $W(L/2,t)/W_0$ of the beam in a 3D space consists of three directions (time parameter vt/L, the velocity parameter $S_1 = \pi v/\omega_1 L$, and another upward direction for the impact factor (relative displacement) $W(L/2,t)/W_0$ in Figure 6(a). Furthermore, Figure 6(b) presents a top-down view of Figure 6(a). In addition, Figure 6 provides a general illustration of the effect of time and vehicle velocity parameters on the dynamic behaviour of the bridge.

Figure 7 shows the intersection of planes perpendicular to the velocity axis and their cross-section for values S_1=0,0.3,0.5,1 and 2, which intersect the graphical evolution of relative displacements according to curves representing the temporal evolution of the beam displacement.

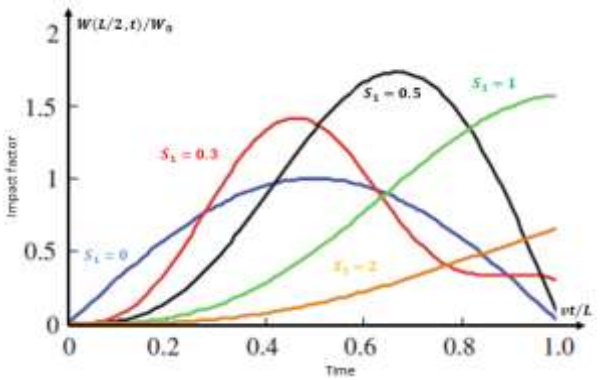

Fig. 7: The impact factor at mid-span of the bridge for different speeds of the suspended mass

From Figure 7, we can see that at very high speed the maximum dynamic displacement occurs when the suspended mass leaves the bridge. As the speed of the load decreases, the peak (the maximum relative displacement) appears when the suspended mass is close to the centre of the beam. By progressively increasing the speed, the position of the load producing the maximum dynamic displacement at mid-span moves towards the end of the bridge.

5.3 Dynamics of the Bridge under a Train Loading

During the dynamic analysis of the interactions between the two subsystems, the train can be modeled as a sequence of (N=10 wheels) suspended masses (moving at a constant velocity v) separated from each other by uniform distances equal to the length of each railcar d_v (other properties and parameters are presented in Table 1), as shown in Figure 3.

The curves shown in Figure 8 are obtained after a numerical study of the mathematical formulation of Section 2. Using the small deformation approximation, the displacement of the beam will be obtained by the principle of superposition of all

the responses induced by individual suspended masses, such as:

$$W_b(x,t) = \sum_{k=0}^{N-1} W_{bk}(x,\ t - \frac{kd_v}{v}) \quad (33)$$

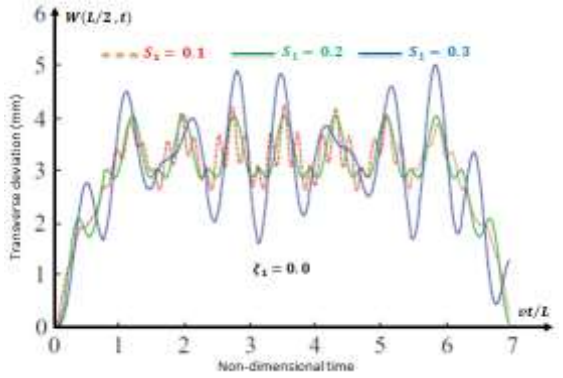

(a)

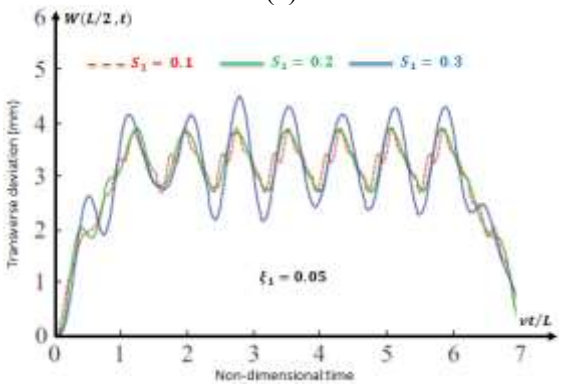

(b)

Fig. 8: The impact factor of the mid-span bridge as a function of time for a series of 10 loads (a) damping factor ξ_1=0.0 (b) damping factor ξ_1=0.05

By manipulating the method described above, the transverse deflection at mid-span of a beam with a span of $L = 34\ m$, simply supported at its edges, is obtained. With a fundamental frequency (for the first mode), (Table 3) $\omega_1 = 30.05 \frac{rad}{s}$, the study is conducted in two damping situations $\xi_1 = 0.0\ and\ \xi_1 = 0.05$. The time evolution of relative displacements illustrated in Figure 8(a) and Figure 8(b) shows several maximum values depending on the combinations of the effects of the exciting loads on the beam. Damping has the effect of stabilizing the vibrations of the bridge.

In the last section of the proposed study, we consider a bridge schematized as a pre-stressed concrete beam with simple supports at the boundaries, and its properties are as follows.

In Figure 9, we present the impact factor $IF = W(L/2,t)/W_0$ for the displacement of the mid-point of the bridge excited by the series of suspended masses as a function of the first velocity parameter $S_1 = \pi v/\omega_1 L$. The parameter S_1 is defined as the ratio between the excitation frequency of the moving train $\pi v/L$ and the first (fundamental) frequency ω_1 of the bridge. The form of irregularity proposed in this study is the one adopted by [24] and is expressed as follows.

$$r(x) = -\frac{5}{10^4}\left(1 - e^{-x^3}\right)\sin(2\pi x) \quad (34)$$

Table 3. Beam Properties

$L\ (m)$	$A\ (m^2)$	$I_z\ (m^4)$	$m_b\ \left(\frac{kg}{m}\right)$	Fréquences en rad/s		Liaisons aux frontières
34	8	10.3	32562	$\omega_1 = 30.05$	$\omega_2 = 145.2$	Appui simple

Crossed by a train characterized by the following parameters (Table 4).

Table 4. Technical properties of the train

$d_v\ (m)$	$M_v\ (kg)$	$m_v\ (kg)$	$k_v\ (kN/m)$	$c_v\ (kN-s/m)$
20	20000	0	1600	76

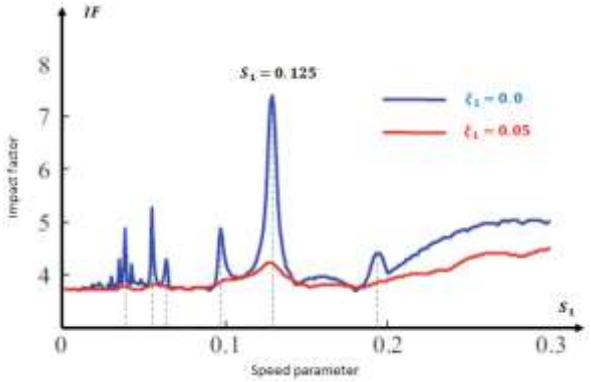

Fig. 9: Maximum impact factor at mid-range as a function of the speed parameter for two damping ratios

We observe that the successive periodic effects of the train wheels action induce multiple peaks of relative displacements. These peaks indicate resonant responses of the beam. Therefore, the largest peak of the impact factor (dynamic relative displacement) is produced at $S_1 = 0.125$, which corresponds to a train speed of $v = 146{,}35\frac{km}{h}$. Furthermore, considering damping, the maximum displacement will be reduced, and consequently, the resonant response. This result is consistent with the work under the passage of a single HS20-44 truck, [25].

6 Conclusion

It is important to note that dynamic loads only cause minor damage to the bridge, such as the resonance phenomenon (with damping, resonance may have a negligible effect), but they result in continuous deterioration of the bridge, increasing maintenance needs. Examining how these factors affect the bridge's response is crucial for operating costs. To better understand the structural behavior, the results of several parametric studies have been presented. Furthermore, as the suspended mass behaves in some ways like a mass applied to the bridge, the inclusion of the inertial effect of moving vehicles, represented by the suspended mass model, has led to a slight reduction in the maximum bridge response. Additionally, it is very clear that the harder the ballast (with significant rigidity), the higher the train speed at which the resonance phenomenon is triggered. The rigidity of the moving vehicle suspension system has a negligible effect when determining bridge dynamics as the objective. The results mentioned above pertain to bridge safety but not to vehicle dynamics and, therefore, passenger comfort.

Acknowledgements:
The authors would like to thank sidi Mohammed ben Abdellah University for supporting this work. The authors also thank the professors of the "ENS" Fez for their assistance in manuscript correction.

References:

[1] Zou Q., Deng L., Guo T. and Yin X. (2016); Comparative Study of Different Numerical Models for Vehicle–Bridge Interaction Analysis; *International Journal of Structural Stability and Dynamics* Vol. 16, No. 09, 1550057; https://doi.org/10.1142/S021945541 5500571

[2] Zenunovic D., Topalovic M. and Folic, R. (2015); Identification of Modal Parameters of Bridges Using Ambient Vibration Measurements; *Shock and Vibration* Article ID 957841,1–21; https://doi.org/10.1155/2015/957841.

[3] Chen G.W., Omenzetter P. and Beskhyroun S. (2021); Modal systems identification of an eleven-span concrete motorway off-ramp bridge using various excitations; *Engineering Structures* 229 111604, https://doi.org/10.1016/j.engstruct.2020.111604/.

[4] Szafranski M. (2021); A dynamic vehicle-bridge model based on the modal identification results of an existing EN57 train and bridge spans with non-ballasted tracks; *Mechanical Systems and Signal Processing* 146 107039; https://doi.org/10.1016/j.ymssp.2020.107039.

[5] Kużawa M., Mroz A. and Bień J. (2022); Influence of Permanent Deflections on The Vibrations of Bridge Spans in Operating Conditions; *Studia Geotechnica et Mechanica*, 44, 1–17; https://doi.org/10.2478/sgem-2022-0004.

[6] Stoura C. D. and Dimitrakopoulos E. G. (2020); Additional damping effect on bridges because of vehicle-bridge interaction; *Journal of Sound and Vibration*, 476, 115294; http://doi:10.1016/j.jsv.2020.115294.

[7] Yang Y. B., Zhang B., Qian Y. and Wu Y. (2018); Contact-Point Response for Modal Identification of Bridges by a Moving Test Vehicle; *International Journal of Structural Stability and Dynamics*, 18(05), 1850073; https://doi.org/10.1142/S0219455418500736

[8] Xie Q., Han W. and Yuan, Y. (2020); Refined Vehicle-Bridge Interaction Analysis Using Incompatible Solid Finite Element for Evaluating Stresses and Impact Factors; *Advances in Civil Engineering*, 1–15; https://doi.org/10.1155/2020/7032460.

[9] Kilikevicius A., Bacinskas D., Selech J., Matijošius J., Kilikeviciene K., Vainorius D., Ulbrich D. and Romek D. (2020); The Influence of Different Loads on the Footbridge Dynamic Parameters; *Mechanical Engineering* 12 (4), 657; https://doi.org/10.3390/sym12040657.

[10] Eshkevari S. S., Matarazzo T. J. and Pakzad S. N. (2020) ; Simplified Vehicle-Bridge Interaction for Medium to Long-span Bridges Subject to Random Traffic Load; *Journal of Civil Structural Health Monitoring*, vol. 10, pages 693–707, https://doi.org/10.1007/s13349-020-00413-4.

[11] Sun Y. Q., Cole C., Spiryagin M. and Dhanasekar M. (2013); vertical dynamic interaction of trains and rail steel bridges; *Electronic Journal of Structural Engineering* 13(1): 88-97; http://dx.doi.org/10.56748/ejse.131641.

[12] Yang Y. B., Yau J. D. and Yang Y. B. (2004); vehicle-bridge interaction dynamics: with applications to high-speed railways; *World Scientific Publishing Co.* Pte. Ltd. ISBN 981-238-847-8.

[13] Stoura C. D. and Dimitrakopoulos E. G. (2021); effect of vehicle-bridge-interaction on the vibration of the bridge; *14th World Congress on Computational Mechanics (WCCM), Conference: 14th WCCM-ECCOMAS* Congress; http://dx.doi.org/10.23967/wccmeccomas.2020.127.

[14] Yang Y. B., Zhang B., Qian Y. and Wu Y. (2017); Contact-Point Response for Modal Identification of Bridges by a Moving Test Vehicle; *International Journal of Structural Stability and Dynamics*, 18(05), 1850073; https://doi.org/10.1142/S0219455418500736.

[15] Zeng Q., Yang Y.B. and Dimitrakopoulos E.G. (2016); Dynamic response of high-speed vehicles and sustaining curved bridges under conditions of resonance; *Engineering Structures*, 114 61–74; http://doi:10.1016/j.eng struct.2016.02.006.

[16] Ferreira A.J.M. (2009); *MATLAB Codes for Finite Element Analysis*; Library of Congress Control Number: 2008935506, ISBN: 978-1-4020-9199-5.

[17] Cantero D., Hester D. and Brownjohn J. (2017); Evolution of bridge frequencies and modes of vibration during truck passage; *Engineering Structures*, 152 452 64; https://doi.org/10.1016/j.engstruct.2017.09.039.

[18] He X., Wu T., Zou Y., Chen Y. F., Guo H. and Yu Z. (2017); Recent developments of high-speed railway bridges in China; *Structure and Infrastructure Engineering*, 13(12), 1584–1595; doi:10.1080/15732479.2017.1304429.

[19] Cantero D., McGetrick P., Kim C.W. and OBrien E. (2019); Experimental monitoring of bridge frequency evolution during the passage of vehicles with different suspension properties; *Engineering Structures*, 187 209–219; http://doi:10.1016/j.engstruct.2019.02.065.

[20] Stoura C. D. and Dimitrakopoulos E. G. (2020); Additional damping effect on bridges because of vehicle-bridge interaction; *Journal of Sound and Vibration*, 115294; http://doi:10.1016/j.jsv.2020.115294.

[21] Karl Popp and Werner Schiehlen (2010); Ground Vehicle Dynamics; Springer-Verlag Berlin Heidelberg ISBN 978-3-540-24038-9; https://doi.10.1007/978-3-540-68553-1.

[22] He Xia, Nan Zhang, Weiwei Guo (2018); Dynamic Interaction of Train-Bridge Systems in High-Speed Railways Theory and Applications; *Library of Congress Control* Number: 2017940357, ISBN 978-3-662-54869-1; https://doi.org/10.1007/978-3-662-54871-4.

[23] H. Xia, G. De Roeck and Jose M. Goicolea (2012); Bridge Vibration and Controls; by *Nova Science Publishers*, Inc., ISBN: 978-1-62100-905-4

[24] Nielsen J. C. O. and Abrahamsson T. J. S. (1992); Coupling of physical and modal components for analysis of moving non-linear dynamic systems on general beam

structures; *International Journal for Numerical Methods in Engineering* 33(9), 1843-1859, https://doi.org/10.1002/nme.1620330906.

[25] Yang Y.B., Liao S.S. and Lin, B.H. (1995); Impact Formulas for Vehicles Moving over Simple and Continuous Beams; Journal of Structural Engineering, 121(11), 1644–1650; 10.1061/(ASCE)0733-9445(1995)121:11(1644).

APPENDIX

The expressions of the Hermite shape functions are:

$$\begin{aligned} N_1(\xi) &= (2-3\xi+\xi^3)/4 \\ N_2(\xi) &= l(1-\xi-\xi^2+\xi^3)/4 \\ N_3(\xi) &= (2+3\xi-\xi^3)/4 \\ N_4(\xi) &= l(-1-\xi+\xi^2+\xi^3)/4 \end{aligned} \quad \text{(A-1)}$$

"Let the element « e » with length « l » be as follows:

The mass and stiffness matrices of each element are:

$$[m_b] = \frac{m_b l}{420}\begin{bmatrix} 156 & 22l & 54 & -13l^2 \\ 22l & 4l^2 & 13l & -3l^2 \\ 54 & 13l & 156 & -22l \\ -13l^2 & -3l^2 & -22l^2 & 4l^2 \end{bmatrix} \quad \text{(A-2)}$$

A beam with a square cross-sectional shape is characterized by a moment of inertia $I = I_y = I_z = \frac{a^4}{12}$, where "a" is the side length of the section.

$$[k_b] = \frac{EI_z}{l^3}\begin{bmatrix} 12 & 6l & -12 & 6l \\ 6l & 4l^2 & -6l & 2l^2 \\ -12 & -6l & 12 & -6l \\ 6l & 2l^2 & -6l & 4l^2 \end{bmatrix} \quad \text{(A-3)}$$

For most cases in civil engineering, it is not cost-effective to consider all modes when calculating the damping matrix $[c_b]$.. In the case where two modes are considered, known as Rayleigh damping, the damping matrix is reduced to

$$[c_b] = \frac{2\xi\omega_1\omega_2}{\omega_1+\omega_2}[m_b] + \frac{2\xi}{\omega_1+\omega_2}[k_b] \quad \text{(A-4)}$$

Where the first natural frequencies of the beam are ω_1 *and* ω_2, let's assume that the damping ratio is ξ1=ξ2=ξ.

Contribution of Individual Authors to the Creation of a Scientific Article (Ghostwriting Policy)

- Ayoub El Amrani and Hafid Mataich carried out the simulation, the optimization and implemented the Algorithm in C++. They discussed the results of the work.
- Bouchta El Amrani supervised all the work.

This work is the work of the group supervised by Professor Bouchta EL AMRANI laboratory of mathematics, modelling and applied physics.

Sources of Funding for Research Presented in a Scientific Article or Scientific Article Itself

No funding was received for conducting this study.

Conflict of Interest

The authors have no conflicts of interest to declare.